# Universality in phase boundary slopes for spin glasses on self dual lattices

Masayuki Ohzeki,[1] Creighton K. Thomas,[2] Helmut G. Katzgraber,[2, 3] H. Bombin,[4] and M. A. Martin-Delgado[5]

[1]*Department of Systems Science, Graduate School of Informatics,*
*Kyoto University, Yoshida-Honmachi, Sakyo-ku, Kyoto 606-8501, Japan*
[2]*Department of Physics and Astronomy, Texas A&M University, College Station, Texas 77843-4242, USA*
[3]*Theoretische Physik, ETH Zurich, CH-8093 Zurich, Switzerland*
[4]*Perimeter Institute for Theoretical Physics, Waterloo, Ontario N2L 2Y5, Canada*
[5]*Departamento de Física Teórica I, Universidad Complutense, 28040 Madrid, Spain*
(Dated: February 2, 2011)

We study the effects of disorder on the slope of the disorder–temperature phase boundary near the Onsager point ($T_c = 2.269\ldots$) in spin-glass models. So far, studies have focused on marginal or irrelevant cases of disorder. Using duality arguments, as well as exact Pfaffian techniques we reproduce these analytical estimates. In addition, we obtain different estimates for spin-glass models on hierarchical lattices where the effects of disorder are relevant. We show that the phase-boundary slope near the Onsager point can be used to probe for the relevance of disorder effects.

PACS numbers: 75.50.Lk, 75.40.Mg, 05.50.+q, 64.60.-i

## I. INTRODUCTION

The critical behavior of lattice spin systems can change drastically when disorder is introduced. Harris [1] demonstrated that whenever $2 - d\nu < 0$ ($d$ the space dimension, $\nu$ the critical exponent of the correlation length) the universality class of the system *without* disorder can change when disorder is introduced [2]. The two-dimensional Ising model [3]—one of the simplest yet nontrivial classical spin systems—has $d\nu = 2$. When disorder is added one obtains the two-dimensional Edwards-Anderson Ising spin glass [4, 5]. However, the model is marginal in that the disorder only changes the singularity in the specific heat from a logarithmic to a double-logarithmic behavior [6, 7]. Different numerical studies have addressed this problem on square lattices [8–11], however, a detailed study of the gradual increase of the perturbation of the system on non-Bravais lattices remains to be performed.

In this work we study the effects of a gradual increase of the disorder for small disorder perturbations for the two-dimensional Ising model on different lattice geometries and, in particular, non-Bravais lattices. We study the slope of the phase boundary of the disorder–temperature phase diagram in the limit of vanishing disorder as a means to detect if disorder is a relevant perturbation or not.

The phase-boundary slope of the two-dimensional bond-diluted Ising model has been studied in detail by different research groups [12–14]. In particular, Domany's perturbative approach gives an "exact" result for the slope in the case of the bond-diluted Ising model, as well as the Ising model with bimodal disorder on square lattices [14, 15]. The results stems from a simple perturbation technique combined with duality arguments, as well as the replica method. The effective Hamiltonian is separated into two parts: a nonrandom replicated Ising model and an operator representing the effects of the disorder that corresponds to interactions among dif-ferent replicas. The analysis, starting from this effective Hamiltonian, is validated when the effects of the disorder are not relevant from a renormalization-group perspective. Note that this approach can be applied to any self-dual lattice as long as one assumes that *the disorder does not affect the nature of the critical behavior.*

Therefore, the value of the slope has certain universal properties shared within the self-duality and the irrelevant disorder. Despite nonanalyticities known to be present in disordered Ising models [16], the disorder seems to merely give rise to a linear shift in the critical point (for small disorder), because most relevant operators in the disordered part of the effective Hamiltonian are marginal in two dimensions. Therefore, a naive perturbation that evaluates only the shift of the critical point without any further consideration can be justified and would give an exact value of the slope of the phase boundary near the critical temperature in the zero-disorder limit. For the case of the two-dimensional Ising model on the square lattice, this would be the Onsager point $[T_c^{\mathrm{IM}} = 2/\ln(1 + \sqrt{2}) \approx 2.26918\ldots]$ [17, 18]. However, it is unclear if this is still valid when the disorder is a relevant perturbation.

In this work we compute the phase boundary slope for different self-dual lattices using duality arguments [19, 20]. We can therefore infer from the value of the phase boundary slope if the disorder is a relevant perturbation or not: If the obtained results do not agree with Domany's prediction, we can infer that the disorder is a relevant perturbation. Finally, we compare these results to the phase boundary slope of the two-dimensional Ising model with bimodal disorder computed using exact Pfaffian methods [21], also validated via Monte Carlo data.

## II. HIERARCHICAL LATTICES

Because considerably larger system sizes can be computed using hierarchical lattices, we first analyze the

phase-boundary slope on self-dual hierarchical lattices using the duality approach introduced in Ref. [19]. Due to the self-duality [17] of the hierarchical lattices, the critical point is the same as for the two-dimensional Ising model on the square lattice. However the relevance of the disorder can change depending on the geometry of the hierarchical lattice [22].

### A. Review: Duality analysis for spin glasses

We first outline the duality analysis expanded to spin glasses. The goal is to study the phase boundary of the bond-diluted and bimodal Ising model in two space dimensions given by the Hamiltonian

$$\mathcal{H} = -J \sum_{\langle ij \rangle} \tau_{ij} S_i S_j. \tag{1}$$

Here $S_i$ represent Ising spins and the sum is over nearest neighbors. $J$ defines the energy scale. For convenience, the partition function is written as a function of the coupling constant $K = \beta J$ ($\beta = 1/T$, $T$ the temperature):

$$Z(K) = \sum_{\{S_i\}} \prod_{\langle ij \rangle} e^{K \tau_{ij} S_i S_j}, \tag{2}$$

where the couplings $\tau_{ij}$ are given by

$$P(\tau_{ij}) = p\delta(\tau_{ij} - 1) + (1 - p)\delta(\tau_{ij} + 1) \tag{3}$$

for the two-dimensional Ising model with bimodal disorder and

$$P(\tau_{ij}) = p\delta(\tau_{ij} - 1) + (1 - p)\delta(\tau_{ij}) \tag{4}$$

for the bond-diluted version of the model. For $p = 1$ the standard duality analysis can be applied [17, 23] to obtain the exact location of the Onsager point (without having to evaluate the free energy) by relating two partition functions at different temperatures, i.e.,

$$Z(K) = \lambda^{N_B} Z(K^*). \tag{5}$$

Here $N_B$ is the number of bonds and $\lambda = [1 + \exp(-2K)]/\sqrt{2}$ is a ratio of the local principal Boltzmann factors when the edge spins are parallel, i.e., $x_0 = \exp(K)$ and its dual $x_0^* = [\exp(K) + \exp(-K)]/\sqrt{2}$. The dual coupling constant is given by $K^* = -\ln(\tanh K)/2$. Under the assumption that there is a single transition temperature, we identify the critical point by the condition $K = K^* \equiv K_c$, i.e., the Onsager point [17, 18, 23]. In this case the prefactor $\lambda$ then becomes unity.

However, when disorder is present, a replica approach has to be included to determine the critical point. In this case the effective partition function is given by

$$Z_n(\{x\}) = \left[ \sum_{\{S_i^{(\alpha)}\}} \prod_{\alpha=1}^{n} \prod_{\langle ij \rangle} e^{K \tau_{ij} S_i^{(\alpha)} S_j^{(\alpha)}} \right]_{\text{av}}, \tag{6}$$

where $n$ is the replica number, and $[\cdots]_{\text{av}}$ represents an average over the disorder. A similar relation as in Eq. (5) can be derived, namely

$$Z_n(\{x\}) = \lambda_n^{N_B} Z_n(\{x^*\}). \tag{7}$$

Instead of the relationship between low and high temperatures as in the case without disorder we establish a duality relation between the local Boltzmann factors $x_k$ and $x_k^*$ [20, 24, 25], where $k$ denotes the number of anti-parallel pairs in $n$-replicated bonds. The important local principal Boltzmann factor is the one with the edge spins parallel, i.e., $x_0 = [\exp(nK\tau_{ij})]_{\text{av}}$; the dual one is $x_0^* = [(\exp(K\tau_{ij}) + \exp(-K\tau_{ij}))/\sqrt{2}\}^n]_{\text{av}}$ given by the 2-component Fourier transform in par with standard duality procedures [23]. It follows that $\lambda_n = x_0^*/x_0$.

Because the traditional duality arguments to find a fixed point in an arbitrary replica number give unphysical results, we establish the hypothesis that the prefactor $\lambda_n$ should be unity at the critical point also for the case of spin glasses [24, 25]. This assumption is verified as correct by comparing results for different critical points to results from other methods.

Recently, in Ref. [20] an improvement of this approach has been proposed where one considers finite-size clusters to regularly sum over a subsection of spins on the square lattice as a real-space renormalization after the ordinary duality transformation, see Fig. 1. This accounts better for the effects of the quenched randomness. Using this approach one obtains:

$$Z_n^{(s)}(\{x^{(s)}\}) = \left( \lambda_n^{(s)} \right)^{N_B/N_B^{(s)}} Z_n^{(s)}(\{x^{*(s)}\}), \tag{8}$$

where $N_B^{(s)}$ is the number of bonds in the cluster, and $s$ denotes the size of the cluster. The partition function is no longer written by simple two-body interactions because of a regular summation which we denote as $Z^{(s)}$ and $Z^{*(s)}$. The local Boltzmann factors $\{x\}$ and $\{x^*\}$ are modified by a regular summation into $\{x^{(s)}\}$ and $\{x^{*(s)}\}$, which represents these many-body interactions. The prefactor is also changed to $\lambda_n^{(s)} = x_0^{*(s)}/x_0^{(s)}$, which is the ratio of the renormalized principal Boltzmann factors with the spins on the perimeter of the cluster fixed, as shown in Fig. 1 (fixed spins are represented by open circles).

A single equality—$\lambda_n^{(s)} = 1$—then gives a more precise location of the critical point in comparison to the standard duality approach because the effects of the disorder are properly included.

The precision of critical points determined with the improved duality approach increases with increasing cluster size, similar to a renormalization-group analysis. When the studied lattice can be built via a recursion—as in the case of hierarchical lattices [26, 27]—the real-space renormalization group analysis (the regular summation over a part of spins in each step of the renormalization) can yield exact results asymptotically for the partition function and related quantities [19]. In this case the cluster
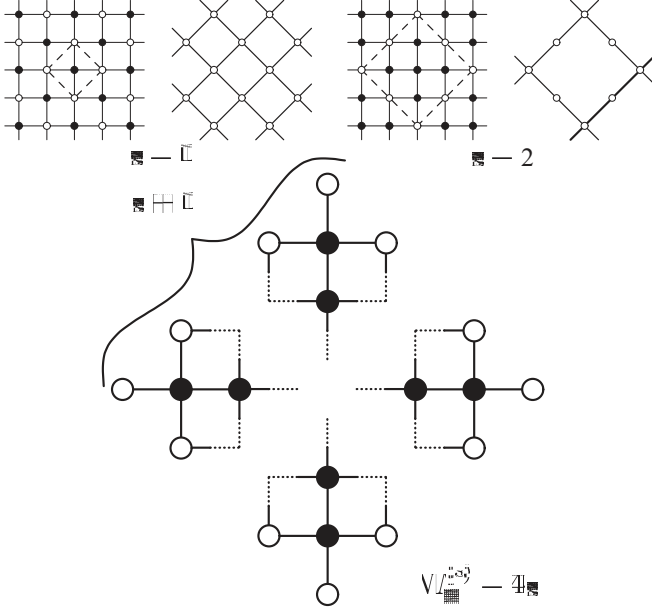
FIG. 1: Clusters used in the summation over a subset of spins on a square lattice for the improved duality approach. The full circles represent the spins summed over, while the white circles are treated as fixed.
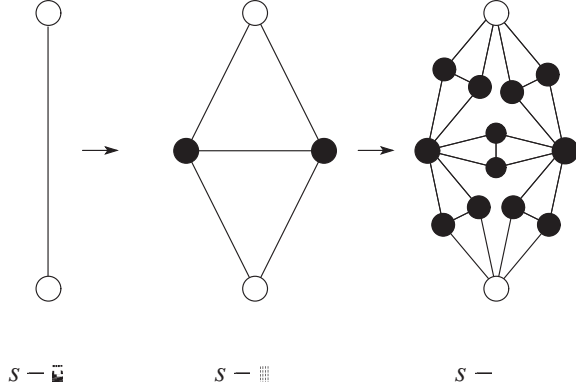


FIG. 2: Self-dual hierarchical lattice. Full circles represent spins summed over while the white circles are fixed. The hierarchical lattice is constructed by inserting a unit cell at each bond. The renormalization corresponds exactly to the inverse process.

size $s$ represents the number of the step in the construction instead of the cluster size, as shown in Fig. 2.

The prefactor $\lambda_n^{(s)}$ is explicitly given by the ratio of $x_0^{(s)} = [Z_{\rm cl}^{(s)}(K)^n]_{\rm av}$ and $x_0^{*(s)} = [Z_{\rm cl}^{*(s)}(K)^n]_{\rm av}$, where $Z_{\rm cl}(K)$ represents the standard partition function as in Eq. (2) but limited to the cluster, and $Z^*(K)$ is its dual. The principal Boltzmann factors $x_0^{(s)}$ and $x_0^{*(s)}$ can be

regarded as the $n$-replicated partition function on the finite-size cluster after a configurational (disorder) average. The quenched (replica) limit $n \to 0$ of $\lambda_n^{(s)}$ yields an equation that allows for the determination of the critical points of spin glasses, namely

$$\left[\log Z_{\rm cl}^{*(s)}(K)\right]_{\rm av} - \left[\log Z_{\rm cl}^{(s)}(K)\right]_{\rm av} = 0. \qquad (9)$$

Starting from this equation, for instance, one can compute to high precision the location of the multicritical point for the bimodal ($\pm J$) Ising model ($p_c = 0.89082$) using the $s = 2$ cluster on the square lattice. This also proves that there is no finite-temperature spin-glass transition when the disorder distribution is symmetric ($p = 0.5$) on *any* self-dual lattice in two space dimensions [20, 28].

## B.  Computing phase-boundary slopes

In the present study we estimate the value of the critical phase boundary slope near the Onsager point for the bimodal ($\pm J$) Ising model and the bond-diluted Ising model. After that, we compare our results with the standard perturbation result for the bimodal case by Domany for the phase boundary slope $\zeta$, namely [14]

$$\zeta \equiv \frac{1}{T_c^{\rm IM}} \left.\frac{\Delta T}{\Delta p}\right|_{p\to 0} = \frac{1}{K_c \langle \sigma_i \sigma_j \rangle_{K_c}} = 3.2091\ldots, \quad (10)$$

where $\langle \sigma_i \sigma_j \rangle_{K_c}$ is the correlator between nearest-neighbor spins, which is the same as the internal energy divided by the number of bonds. $T_c^{\rm IM} = 2/\ln(1 + \sqrt{2}) \approx 2.26918$ is the critical temperature of the two-dimensional Ising model without disorder [17, 18] shared within the self-dual hierarchical lattices. To compute the slope of the phase boundary close to the Onsager point we expand Eq. (9) to first order for $\Delta p \ll 1$

$$\left(1 - N_B^{(s)}\Delta p\right)\left(\log Z_0^{*(s)}(K) - \log Z_0^{(s)}(K)\right)$$
$$+\Delta p \sum \left(\log Z_1^{*(s)}(K) - \log Z_1^{(s)}(K)\right) = 0. (11)$$

Here $N_B^{(s)}$ denotes the number of bonds on the finite-size cluster. For the bimodal ($\pm J$) Ising model, $Z_0$ and $Z_0^*$ are the partition functions without any antiferromagnetic interactions (or without absence of interactions for the bond-diluted Ising model). $Z_1$ and $Z_1^*$ are those with a single antiferromagnetic interaction (or absence of interactions for the bond-diluted Ising model). The summation (reduced configurational average for $\tau_{ij}$) is taken over all realizations with a single antiferromagnetic interaction on the cluster. Next, we set the coupling constant as $K_c + \Delta K$ ($\Delta K \ll 1$) near the Onsager point. Equation (11) for the slope $\zeta$ thus reduces to

$$\zeta \equiv \frac{1}{T_c^{\mathrm{IM}}} \left.\frac{\Delta T}{\Delta p}\right|_{p \to 0} = \frac{Z_0^{(s)}(K_c)}{K_c} \sum \left( \log Z_1^{*(s)}(K_c) - \log Z_1^{(s)}(K_c) \right) \left( \frac{\mathrm{d}Z_0^{*(s)}}{\mathrm{d}K} - \frac{\mathrm{d}Z_0^{(s)}}{\mathrm{d}K} \right)^{-1}, \tag{12}$$
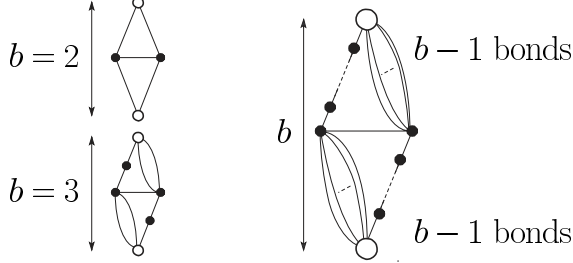


FIG. 3: Unit cells of the self-dual hierarchical lattices. $b$ is the length of the unit size of the hierarchical lattice.

where we use the identity $Z_0^*(K_c) = Z_0(K_c)$ at the On-sager point [see Eq. (5)]. To estimate the precise value of the slope we need to compute the exact value of the partition function on the finite-size cluster and evaluate the reduced configurational average over all the possible locations of a single antiferromagnetic interaction. The precision of the slope computation depends on the finite-size cluster used. This, in turn, depends on the evaluation of the partition function and the reduced configuration average, all scaling $\sim \mathcal{O}(N_B^{(s)})$ for the hierarchical lattices. If the calculation converges with an increasing number of bonds we can estimate the thermodynamic limit value to high precision by a simple extrapolation.

### C. Results

On the hierarchical lattice (Fig. 3) a simple iterative recursion can be used to estimate the partition function exactly [26, 27]. We can thus obtain an estimate of the slope by studying sufficiently-large clusters using Eq. (12). At each step of the renormalization an estimate is obtained for a given cluster size. Results for both bimodal and bond-diluted disorder are shown in Tables I, II, and III, respectively. The data clearly converge to a definite value.

For the hierarchical lattice with $b = 2$ we sum up spins up to $N_B^{(s=17)} = 5^{17}$. Equation (12) for the bimodal Ising model yields $3.209112646897937\ldots$ for the phase boundary slope, in agreement (up to 13 digits) with the simple perturbative approach of Domany [$3.209112646897908\ldots$]. For the bond-diluted Ising model we obtain for the phase boundary slope $1.3292579815281371\ldots$ using the duality approach; the simple perturbative approach of Domany yields $1.3292579815281351\ldots$ (agreement up to 14 digits). Summarizing, for the $b = 2$ self-dual hierarchical

TABLE I: Results for the phase boundary slope close to the Onsager point for the (bimodal) $\pm J$ and bond-diluted Ising model on the $b = 2$ self-dual hierarchical lattice. The bottom line (marked with 'ED') is computed using the simple perturbative approach by Domany [14, 15].

| $s$ | $\pm J$ | bond diluted |
|---|---|---|
| 1 | 3.238670311607941 | 1.3313280689632047 |
| 2 | 3.213721581962695 | 1.3295847287696935 |
| 3 | 3.209840157687296 | 1.3293096628059718 |
| 4 | 3.209227717235686 | 1.3292661587550924 |
| 5 | 3.209130853824536 | 1.3292592754393175 |
| 6 | 3.209115527844001 | 1.3292581862702618 |
| 7 | 3.209113102764629 | 1.3292580139255745 |
| 8 | 3.209112719032133 | 1.3292579866545563 |
| 9 | 3.209112658312095 | 1.3292579823393163 |
| 10 | 3.209112648704037 | 1.3292579816564926 |
| 11 | 3.209112647183702 | 1.3292579815484458 |
| 12 | 3.209112646943131 | 1.3292579815313489 |
| 13 | 3.209112646905064 | 1.3292579815286436 |
| 14 | 3.209112646899041 | 1.3292579815282155 |
| 15 | 3.209112646898088 | 1.3292579815281478 |
| ED | 3.209112646897908 | 1.3292579815281351 |

TABLE II: Results for the phase boundary slope close to the Onsager point for the (bimodal) $\pm J$ and bond-diluted Ising model on the $b = 3$ self-dual hierarchical lattice. The bottom line (marked with 'ED') is computed using the simple perturbative approach by Domany [14, 15].

| $b = 3$ | $\pm J$ | bond diluted |
|---|---|---|
| 1 | 3.287620710287408 | 1.3346666036511970 |
| 2 | 3.279280357814356 | 1.3341234975081161 |
| 3 | 3.278702594934052 | 1.3340857362686508 |
| 4 | 3.278662410902251 | 1.3340831090945090 |
| 5 | 3.278659615086040 | 1.3340829263029411 |
| 6 | 3.278659420560328 | 1.3340829135847418 |
| 7 | 3.278659407025692 | 1.3340829126998396 |
| 8 | 3.278659406083984 | 1.3340829126382702 |
| 9 | 3.278659406018462 | 1.3340829126339864 |
| 10 | 3.278659406013903 | 1.3340829126336883 |
| 11 | 3.278659406013586 | 1.3340829126336676 |
| ED | 3.209112646897908 | 1.3292579815281351 |

lattices the duality analysis yields results in perfect agreement with the simple perturbative approach.

This implies that the disorder should be marginal or irrelevant on $b = 2$ self-dual hierarchical lattices. However, for $b = 3$ and $b = 4$, estimates of the phase boundary slope using the duality approach disagree with the simple perturbative estimate, see Tables II and III. The simple perturbative result is applicable to all self-dual lattices if we assume that the effect of the disorder operator is

TABLE III: Results for the phase boundary slope close to the Onsager point for the (bimodal) $\pm J$ and bond-diluted Ising model on the $b = 4$ self-dual hierarchical lattice. The bottom line (marked with 'ED') is computed using the simple perturbative approach by Domany [14, 15].

| $s$ | $\pm J$ | bond diluted |
|---|---|---|
| 1 | 3.434735249924405 | 1.3441930333807548 |
| 2 | 3.438341429422663 | 1.3444508638305390 |
| 3 | 3.438917613643436 | 1.3444906297718794 |
| 4 | 3.439007297242741 | 1.3444967410351193 |
| 5 | 3.439021128918736 | 1.3444976788451403 |
| 6 | 3.439023254536054 | 1.3444978226701897 |
| 7 | 3.439023580721387 | 1.3444978447219644 |
| 8 | 3.439023630745810 | 1.3444978481026600 |
| 9 | 3.439023638415719 | 1.3444978486209216 |
| 10 | 3.439023639591570 | 1.3444978487003697 |
| 11 | 3.439023639771829 | 1.3444978487125488 |
| | | |
| ED | 3.209112646897908 | 1.3292579815281351 |
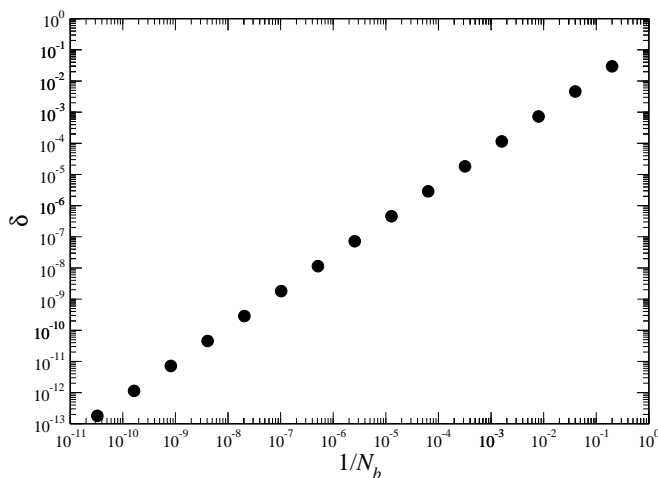


FIG. 4: Difference $\delta$ between the estimate for the slope $\zeta$ from the duality approach [Eq. (12)] and the expected exact result [14] as a function of the cluster size $N_B$ for $b = 2$ self-dual hierarchical lattices. The linear behavior in the log-log plot clearly illustrates the power-law convergence with the system size.

irrelevant. The fact that for the $b = 3$ and $b = 4$ self-dual hierarchical lattices the perturbative and duality methods disagree implies that the disorder operator of the effective Hamiltonian of the bimodal and bond-diluted Ising model is relevant. Furthermore, this suggests that the phase-boundary slope near the Onsager point can be used to probe the relevance of disorder effects.

Finally, our results also show that the data for the slope $\zeta$ converge for an increasing number of bonds to a thermodynamic limiting value as $\zeta(N_B) = \zeta_\infty + a N_B^{-y}$ with $y \approx 1.15$, see Fig. 4 for $b = 2$. The behavior for the other values of $b$ is qualitatively similar.

## III. SQUARE LATTICE

### A. Numerical method

Unfortunately, using the duality analysis on square lattices does not work as well as for hierarchical lattices. Finite-size effects and apparent systematic deviations prevent from an exact determination of the phase-boundary slope in this case. Instead of the duality analysis, we have conducted numerical simulations to compute a precise estimate of the slope $\zeta$ on the square lattice for $p \to 1$ to check the value of Domany.

Pfaffian techniques provide access to exact partition functions in finite spin-glass systems, and developments of these techniques have become quite sophisticated, allowing *exact* results to be computed for larger system sizes and lower temperatures than are accessible with more traditional Monte Carlo techniques [29–31]. Using a dual-lattice approach [31, 32], an algorithm has been recently developed [21] to compute exact correlation functions of the two-dimensional Ising spin glass on the square lattice at all power-of-two length scales in $\mathcal{O}(N^{3/2})$ time for a system of $N = L^2$ spins. The correlation function, $\mathcal{C}(\ell)$, is defined by

$$\mathcal{C}(\ell) = \frac{1}{N_\ell} \sum_{i,j \text{ s.t. } r_{i,j}=\ell} \langle S_i S_j \rangle, \qquad (13)$$

with $r_{i,j}$ being the distance between sites $i$ and $j$, $N_\ell = \sum_{i,j \text{ s.t. } r_{i,j}=\ell} 1$ is the normalization factor, and $\langle \cdots \rangle$ represents an average over the canonical ensemble. We can then construct a dimensionless ratio—similar to the Binder cumulant [33]—for each sample

$$b(\ell_1, \ell_2) = \frac{[\mathcal{C}(\ell_1)]_{\text{av}}}{[\mathcal{C}(\ell_2)]_{\text{av}}}. \qquad (14)$$

In the thermodynamic limit the ferromagnetic state has infinite correlations, i.e., the ratio tends to $b \to 1$ for any pair $\ell_1, \ell_2$, while in the paramagnetic state the correlations die off so that if $\ell_1$ and $\ell_2$ are far apart from one another, they will tend to $b \to 0$ (without loss of generality, assuming that $\ell_1 > \ell_2$). In order to ensure that $\ell_1$ and $\ell_2$ are far apart, it is useful for them both to scale with system size $L$. At the transition temperature $b$ approaches a constant independent of the system size $L$ (up to corrections to scaling). We find empirically that $b(L/2, L/4)$ has very small finite-size corrections, so we use this ratio for our computations.

To extract $T_c$ from the $b$ crossings, we perform a finite-size scaling analysis. It is expected that

$$b \sim \tilde{B}\left(L^{1/\nu}(T - T_c)\right), \qquad (15)$$

where $\tilde{B}$ is a unknown scaling function. The values of $T_c$ and $\nu$ responsible for the best scaling collapse are therefore our best estimates of these quantities.

In order to automatically extract $T_c$ and $\nu$ using standard curve-fitting techniques, we fit to the functional form of $\tilde{B}$. We emphasize that the form of $\tilde{B}$ is unimportant except as a step to automate the procedure: the values we extract for $\nu$ and $T_c$ give a good scaling collapse which may be verified independently (as shown in Fig. 5), and for this purpose the form of $\tilde{B}$ may be discarded. We find that fitting to an arbitrary (four-parameter) cubic polynomial gives a very good scaling collapse. Two independent variables, $L$ and $T$, appear as parameters in $\tilde{B}$. We therefore perform a two-dimensional curve fit using a nonlinear least-squares Levenberg-Marquardt algorithm. To correctly evaluate the statistical error bars, we perform a bootstrap analysis. For each value of $p$ and $T$, we have computed $b$ for $\sim 10^4$ different instances of disorder from which we built a bootstrap sample for the critical parameters [34].

Letting $q \equiv (1 - p)$, simulations have been carried out for $q = 0.0025$ to $0.05$ in increments of $0.025$ up to $N = 128^2$ spins with 10000 disorder samples. The results are summarized in Table IV and Figs. 5 and 6. In Fig. 5 representative scaling collapses of the raw data are presented. For the pure case, $q = 0$, there are no error bars because this is an exact technique. Thus the pure result shows the magnitude of the finite-size effects with this analysis. A sample result at $q = 0.01$ using exchange Monte Carlo is also presented. In this case, the Binder ratio

$$g = \frac{1}{2}\left(3 - \frac{[\langle m^4 \rangle]_{\mathrm{av}}}{[\langle m^2 \rangle]_{\mathrm{av}}^2}\right) \qquad (16)$$

is used. Here $\langle \cdots \rangle$ represents an average over Monte Carlo time. 31 temperatures in the range $[2.0, 2.3]$ are simulated for systems up to $128^2$ spins. The system is equilibrated for $2^{16}$ Monte Carlo sweeps; the same time is used for the time average of the data. Statistical error bars are determined by performing a jackknife analysis of 5000 independent runs. The Binder ratio is expected to follow the same scaling relation [Eq. (15)] as $b$. The Monte Carlo data collapse is not achieved by an additional fit: the values of $T_c$ and $\nu$ extracted for the Pfaffian data are used, illustrating that that an independent numerical method produces consistent results, therefore validating our approach using Pfaffian techniques. For small amounts of disorder ($q < 0.01$), the computed values of $\nu$ are consistent with the pure case of the Ising model where $\nu = 1$ [35], and $\nu$ slowly rises to a value of $\nu \approx 1.10(4)$ for $q = 0.05$. The values of $T_c$ are listed in Table IV. Systematic errors are expected to come primarily from finite-size effects and therefore should be much smaller than the statistical errors. One can then extract a naive slope from each data point by using a finite difference with the known exact value at $q = 0$. These naive slopes are also shown in table IV. This technique does not give a precise estimate of $\zeta$ (we present a precise estimate from a nonlinear curve fit below), but we point out that the slope is steeper than Domany's prediction for every value computed this way. This is due
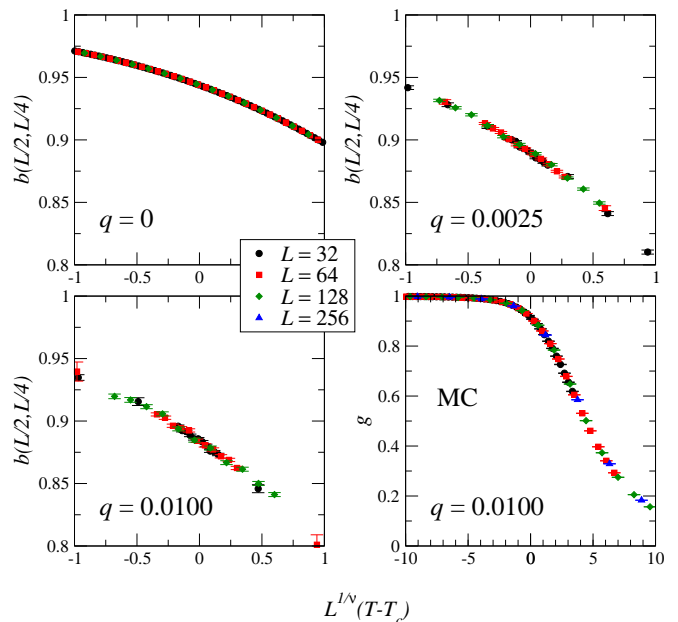


FIG. 5: Finite-size scaling collapse for the ratio $b$ as a function of the scaling variable $L^{1/\nu}(T - T_c)$ for different values of $q$. Representative numerical data used for this scaling collapse are shown for $q = 0$, $0.0025$, and $0.010$. No fitting was done for $q = 0$: the numerical result is exact (no disorder averaging is necessary for $q = 0$), so exactly known values for $T_c$ and $\nu$ in the pure two-dimensional Ising model are used to achieve the data collapse, therefore illustrating that the method used works. The panel on the bottom right labeled with 'MC' is a separate finite-size scaling collapse of the Binder ratio $g$ for independently-computed Monte Carlo data at $q = 0.0100$ using the value of $T_c$ computed for the data in the lower left panel.

to higher-order terms in the small-$q$ expansion.

### B. Results

Our results agree with Domany's value, confirming that this expansion is valid for the two-dimensional Ising model on a square lattice. In Fig. 6 we show the results of a curve fit to a third-order polynomial for the values of $T_c(q)$. We find that linear and quadratic curve fits give high chi-square values and are therefore unlikely to accurately describe the data. We have also carried out curve fits for third-, fourth- and fifth-order polynomials: all three give similar results for the slope, and all three fits have similar chi-square values, implying that the cubic fit gives correct results. The value of the cubic fit is the most precise of these because it has the fewest parameters. The obtained slope from the curve fit is $-3.214(17)/T_c(q = 0)$, which is consistent with Domany's value, while the fit value of $T_c(q = 0)$ is $2.26906(16)$, which is consistent with the known exact result.

TABLE IV: Numerically computed values of $T_c(q)$. In addition, a "naive" estimate of the phase boundary slope near the Onsager point is shown where a linear approximation is performed.

| $q$ | $T_c(q)$ | naive slope |
|---|---|---|
| 0.0025 | 2.25070(11) | 3.258(19) |
| 0.0050 | 2.23261(15) | 3.224(13) |
| 0.0075 | 2.21349(23) | 3.273(14) |
| 0.0100 | 2.19531(22) | 3.256(10) |
| 0.0125 | 2.17670(59) | 3.268(21) |
| 0.0150 | 2.15779(69) | 3.273(20) |
| 0.0175 | 2.13834(48) | 3.295(12) |
| 0.0200 | 2.11852(60) | 3.320(13) |
| 0.0225 | 2.09947(42) | 3.324(8) |
| 0.0250 | 2.08035(41) | 3.329(7) |
| 0.0275 | 2.06058(23) | 3.343(4) |
| 0.0300 | 2.04037(32) | 3.361(5) |
| 0.0325 | 2.02010(35) | 3.378(5) |
| 0.0350 | 1.99970(25) | 3.393(3) |
| 0.0375 | 1.97927(36) | 3.407(4) |
| 0.0400 | 1.95852(77) | 3.423(8) |
| 0.0425 | 1.93790(34) | 3.435(3) |
| 0.0450 | 1.91649(37) | 3.454(4) |
| 0.0475 | 1.89517(59) | 3.470(5) |
| 0.0500 | 1.87265(32) | 3.495(3) |
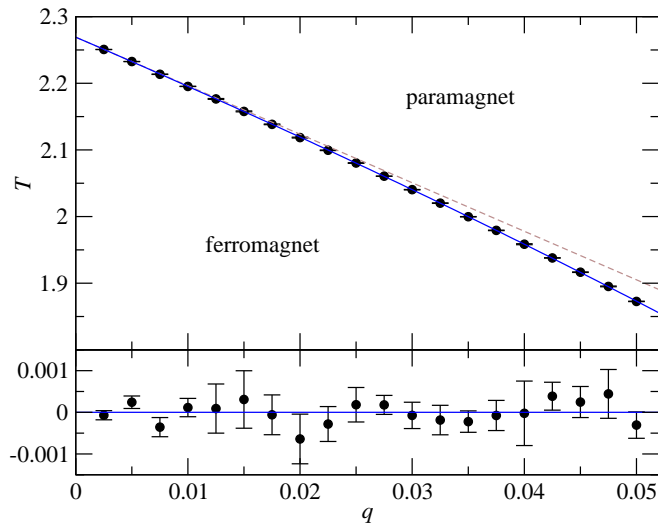


FIG. 6: Top: Numerically-computed phase diagram for $q <$ 0.05. The solid line is the result of a cubic fit to the data. The dashed line is the $q \to 0$ limit given by Domany's value for the slope. Bottom: The residuals of the fit, computed by subtracting the value of the cubic fit from each data point, show no clear trends.

## IV. CONCLUDING REMARKS

The duality analysis on hierarchical lattices shows that the value of the slope is not universal for all the self-dual lattices. This suggests that the simple perturbation theory for the bimodal and bond-diluted Ising model, without paying attention to the relevance of the disorder effects, can yield incorrect results. More generally, our results illustrate that the effects of the disorder can actually modify the value of the slope of the paramagnetic–ferromagnetic phase boundary near the Onsager point for self-dual lattices. For the $b = 2$ self-dual hierarchical lattice the value of the slope agrees with the standard perturbative result by Domany. If the effects of the disorder are relevant, the value of the slope changes depending on the shape of the self-dual lattices sharing the same nonrandom critical point. Therefore, the value of the slope can be regarded as a means for classification of the relevance of the disorder effects on Ising models defined on self-dual lattices. We also numerically reproduce Domany's estimate within statistical error bars for the square lattice using exact Pfaffian techniques.

Several self-dual models where disorder is a relevant operator have a close relationship with topologically-protected quantum computation [36, 37]. It is therefore of interest to gain a deeper understanding of the effects of disorder on self-dual Ising spin systems.

[1] A. B. Harris, J. Phys. C **7**, 1671 (1974).

[2] There are some rare cases where the Harris criterion fails,

such as directed polymers [38] and spin models [22] on hierarchical lattices.

[3] E. Ising, Z. Phys. **31**, 253 (1925).
[4] S. F. Edwards and P. W. Anderson, J. Phys. F: Met. Phys. **5**, 965 (1975).
[5] K. Binder and A. P. Young, Rev. Mod. Phys. **58**, 801 (1986).
[6] V. S. D. Dotsenko and V. Dotsenko, S., Sov. Phys. JETP Lett. **33**, 37 (1981).
[7] V. S. Dotsenko and V. S. Dotsenko, Adv. in Phys. **32**, 129 (1983).
[8] W. L. McMillan, Phys. Rev. B **29**, 4026 (1984).
[9] F. Merz and J. T. Chalker, Phys. Rev. B **65**, 054425 (2002).
[10] M. Picco, A. Honecker, and P. Pujol, J. Stat. Mech. P09006 (2007).
[11] M. Hasenbusch, F. P. Toldin, A. Pelissetto, and E. Vicari, Phys. Rev. E **78**, 011110 (2008).
[12] D. C. Rapaport, J. Phys. C **5**, 1830 (1972).
[13] T. Osawa and K. Sawada, Prog. Theor. Phys. **49**, 83 (1973).
[14] E. Domany, J. Phys. C **12**, L119 (1979).
[15] E. Domany, J. Phys. C **11**, L337 (1978).
[16] R. B. Griffiths, Phys. Rev. Lett. **23**, 17 (1969).
[17] H. A. Kramers and G. H. Wannier, Phys. Rev. **60**, 252 (1941).
[18] L. Onsager, Phys. Rev. **65**, 117 (1944).
[19] M. Ohzeki, H. Nishimori, and A. N. Berker, Phys. Rev. E **77**, 061116 (2008).
[20] M. Ohzeki, Phys. Rev. E **79**, 021129 (2009).
[21] C. K. Thomas and A. A. Middleton, (unpublished).
[22] A. Efrat, Phys. Rev. E **63**, 066112 (2001).
[23] F. Y. Wu and Y. K. Wang, J. Math. Phys. **17**, 439 (1976).
[24] H. Nishimori and K. Nemoto, J. Phys. Soc. Jpn. **71**, 1198 (2002).
[25] J.-M. Maillard, K. Nemoto, and H. Nishimori, J. Phys. A **36**, 9799 (2003).
[26] A. N. Berker and S. Ostlund, J. Phys. C **12**, 4961 (1979).
[27] R. B. Griffiths and M. Kaufman, Phys. Rev. B **26**, 5022 (1982).
[28] M. Ohzeki and H. Nishimori, J. Phys. A **42**, 332001 (2009).
[29] L. Saul and M. Kardar, Phys. Rev. E **48**, R3221 (1993).
[30] A. Galluccio, M. Loebl, and J. Vondrak, Phys. Rev. Lett. **84**, 5924 (2000).
[31] C. K. Thomas and A. A. Middleton, Phys. Rev. E **80**, 046708 (2009).
[32] C. K. Thomas and A. A. Middleton, Phys. Rev. B **76**, 220406(R) (2007).
[33] K. Binder, Phys. Rev. Lett. **47**, 693 (1981).
[34] M. E. J. Newman and G. T. Barkema, *Monte Carlo Methods in Statistical Physics* (Oxford University Press Inc., New York, USA, 1999).
[35] J. M. Yeomans, *Statistical Mechanics of Phase Transitions* (Oxford University Press, Oxford, 1992).
[36] A. Y. Kitaev, Ann. Phys. **303**, 2 (2003).
[37] H. Bombin and M. A. Martin-Delgado, Phys. Rev. Lett. **97**, 180501 (2006).
[38] S. Mukherji and S. M. Bhattacharjee, Phys. Rev. E **52**, 1930 (1995).